Supplementary Information for

Loss of histone H3 K79 methyltransferase Dot1l facilitates kidney fibrosis by upregulating Endothelin 1 through HDAC2

Long Zhang[1, #], Lihe Chen[2, #], Chao Gao[1, #], Enuo Chen[1], Andrea R. Lightle[3], Llewellyn Foulke[3], Bihong Zhao[4], Paul. J. Higgins[1], Wenzheng Zhang[1]

Wenzheng Zhang

e-mail: zhangw1@mail.amc.edu

This PDF file includes:

Supplementary text

Figs. S1 to S6

References for SI reference citations

Supplementary Information

Main Text

Results and Discussion

***Dot1l is* efficiently and specifically disrupted in the CNT/CD of *Dot1l*^{AC} mice.**

To evaluate the efficiency and specificity of *Aqp2Cre*-mediated *Dot1l* ablation, we performed immunofluorescent staining (IF) to examine co-expression of Aqp2 and H3m2K79, a functional indicator of *Dot1l* in various organs. H3m2K79 was readily detectable throughout *Dot1l*$^{f/f}$ kidneys, regardless of Aqp2 expression. In *Dot1l*$^{f/f}$ *Aqp2Cre* (*Dot1l*^{AC}) kidneys, most Aqp2^{+} principal cells and Aqp2^{-} intercalated cells showed no H3m2K79 staining in the cortex and medulla, despite strong H3m2K79 signaling in other Aqp2^{-} tubules/cells (Fig. S1A-B), confirming our earlier work [1]. In other six tissues including brain, both genotypes lacked detectable Aqp2 and had robust H3m2K79 (Fig. S1C-H). To more accurately estimate *Aqp2Cre*-mediated recombination efficiency, we categorized Aqp2^{+} cells into H3m2K79^{+} and H3m2K79^{-} cells. Analyses of 4901 Aqp2^{+} cells from 3 WT kidneys revealed that about 5% cells were scored as H3m2K79^{-}. The percentage of H3m2K79^{-} cells increased dramatically to 98% when 5003 Aqp2^{+} cells from 3 *Dot1l*^{AC} mice were similarly examined (Fig. S1I). These data indicate that *Aqp2Cre* drives Cre-mediated *Dot1l* ablation efficiently and specifically in the CNT/CDs.

***Dot1l* deficiency exacerbates streptozotocin (STZ)-induced kidney fibrosis**

by upregulating ET1. To determine if loss of *Dot1l* function confers susceptibility to DN by upregulating ET1, we studied 4 groups of mice: 1) WT; 2) $Dot1l^{AC}$; 3) DE^{AC} and 4) $Edn1^{AC}$. Mice were sacrificed 4 months post STZ injection. Hematoxylin and Eosin (HE) staining revealed that WT kidneys had neither obvious fibrosis nor tubular atrophy. $Dot1l^{AC}$ mice exhibited focal mesangial expansion and hypercellularity, zonal interstitial fibrosis and tubular atrophy with sparing of glomeruli, consistent with chronic tubulointerstitial injury. These pathological changes were reduced in both DE^{AC} and $Edn1^{AC}$ mice (Fig. S4A). The renal injury score was significantly higher in $Dot1l^{AC}$ than the other three groups (Fig. S4B). The mild fibrosis of all groups may be attributable to their highly pure background of C57BL6, which is relatively resistant to develop severe kidney fibrosis in response to STZ [2].

ImageJ analyses of the Trichrome-stained kidney sections from all strains confirmed that the fibrotic phenotype was significantly more severe in $Dot1l^{AC}$ vs. the others. No significant difference, however, was evident between WT and DE^{AC} or $Edn1^{AC}$ (Fig. S4C-D). This pattern differentiating the 4 groups was also evident in most cases when expression of 6 fibrotic markers (Fibronectin, Fibroblast-specific protein-1 (FSP1), α-SMA, Vimentin, Collagen I, and Collagen IV), ET1, ETA, ETB and HDAC2 (a new Dot1a interactor, see below) and plasma ET1 concentrations were analyzed by RT-qPCR (Fig. S4E-I), immunofluorescence (IF, Fig. S4J), immuoblotting (IB, Fig. S4K-S) and/or enzyme-linked immunosorbent assay (ELISA) (Fig. S4T).

To determine if pathological changes correlated with changes in kidney function, we performed metabolic analyses to measure body weight (BW), water and food intake, 18 urine and blood parameters, and systolic/diastolic BP. Fig. S5 illustrates that *Dot1l*^{AC} vs. WT mice have a significantly higher water intake, urine volume, Na^+ excretion, K^+ excretion, systolic BP, and BUN and lower urine osmolality and [K^+]. The difference in most of these parameters remained significant when *Dot1l*^{AC} mice were compared to *DE*^{AC} or *Edn1*^{AC} animals and became insignificant when *DE*^{AC} or *Edn1*^{AC} were compared to WT mice. All other parameters were not significantly different among the groups, with a few exceptions (Fig. S5). Hence, *Dot1l* plays a renoprotective role in the CNT/CD in the diabetic setting, at least in part by repressing *Edn1*. Since *Edn1*^{AC} mice shared a similar phenotype with WT animals, we focused on the other three groups in the aging and UUO models.

***Dot1l* ablation exacerbates unilateral ureteral obstruction (UUO)-induced kidney fibrosis by upregulating ET1.** It was important to determine if *Dot1l* plays a protective role in UUO-induced renal fibrosis by repressing ET1. For this analysis, WT, *Dot1l*^{AC}, and *DE*^{AC} mice were subjected to UUO and the kidneys removed 14 days post-surgery. While all UUO kidneys, regardless of the genotypes, developed fibrosis with infiltration of inflammatory cells. Trichrome staining signal was significantly higher in *Dot1l*^{AC} vs. WT and *DE*^{AC} animals. *DE*^{AC} and WT controls had comparable levels (Fig. S6A-B). A similar pattern was

observed in most cases for the expression of FSP1, α-SMA, Collagen I, Collagen IV, Fibronectin, Vimentin, ET1, and ETA at mRNA and protein levels (Fig. S6C-M). ETB, nevertheless, became undetectable in each group (data not shown). HDAC2 was significantly elevated in both *Dot1l*^{AC} and *DE*^{AC} mice vs. WT mice (Fig. S6N). Plasma ET1 was mildly higher in *Dot1l*^{AC} vs. WT or *DE*^{AC} mice (Fig. S6O). These results suggest that inactivation of *Dot1l* in the CNT/CD facilitates UUO-induced kidney fibrosis, which can be partially rescued by inactivation of *Edn1*.

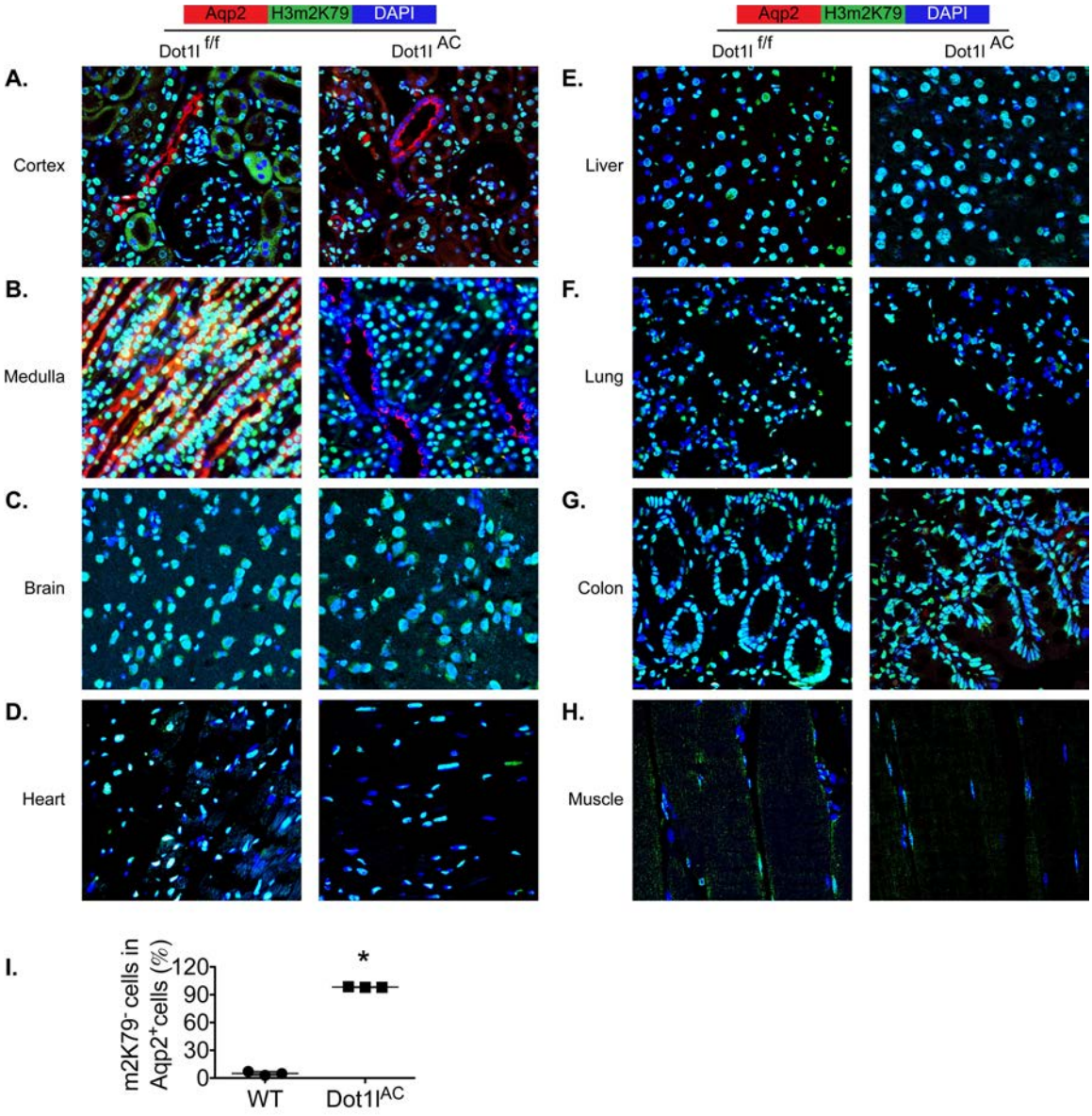
Aqp2
H3m2K79
DAPI
Dot1l f/f
Dot1l AC
A.
Cortex
B.
Medulla
C.
Brain
D.
Heart
E.
Liver
F.
Lung
G.
Colon
H.
Muscle
I.
m2K79- cells in Aqp2+ cells (%)
120
90
60
30
0
*
WT
Dot1lAC

Fig. S1. *Dot1l* is efficiently and specifically disrupted in the CNT/CD of *Dot1l*^{AC} mice. A & **B.** IF images showing strong H3m2K79 (green) throughout the *Dot1l*$^{f/f}$ kidney, regardless of Aqp2 (red) expression, and abolished H3m2K79 in the CNT/CD cells marked by Aqp2 in the cortex and medulla of *Dot1l*^{AC} kidneys. Most of Aqp2-negative intercalated cells in the CNT/CD also had no detectable H3m2K79 since they are derived from Aqp2 lineage during development [1]. Strong H3m2K79 staining in other Aqp2-negative cells/tubules in *Dot1l*^{AC} kidneys were also detected. **C**-**H.** IF images showing undetectable Aqp2 (red) and robust H3m2K79 staining in the organs as indicated in both genotypes. I. Percentage of H3m2K79^{-} cells in Aqp2^{+} cells. About 5000 Aqp2^{+} cells throughout the kidney from each genotype (n=3 mice/genotype) were analyzed. An Aqp2^{+} cell was scored as H3m2K79^{-} if 1) the H3m2K79 signal was undetectable and 2) if DAPI staining showed the presence of the nucleus. An Aqp2^{+} cell with undetectable H3m2K79 staining signal was excluded from quantification if DAPI staining showed the absence of the nucleus.

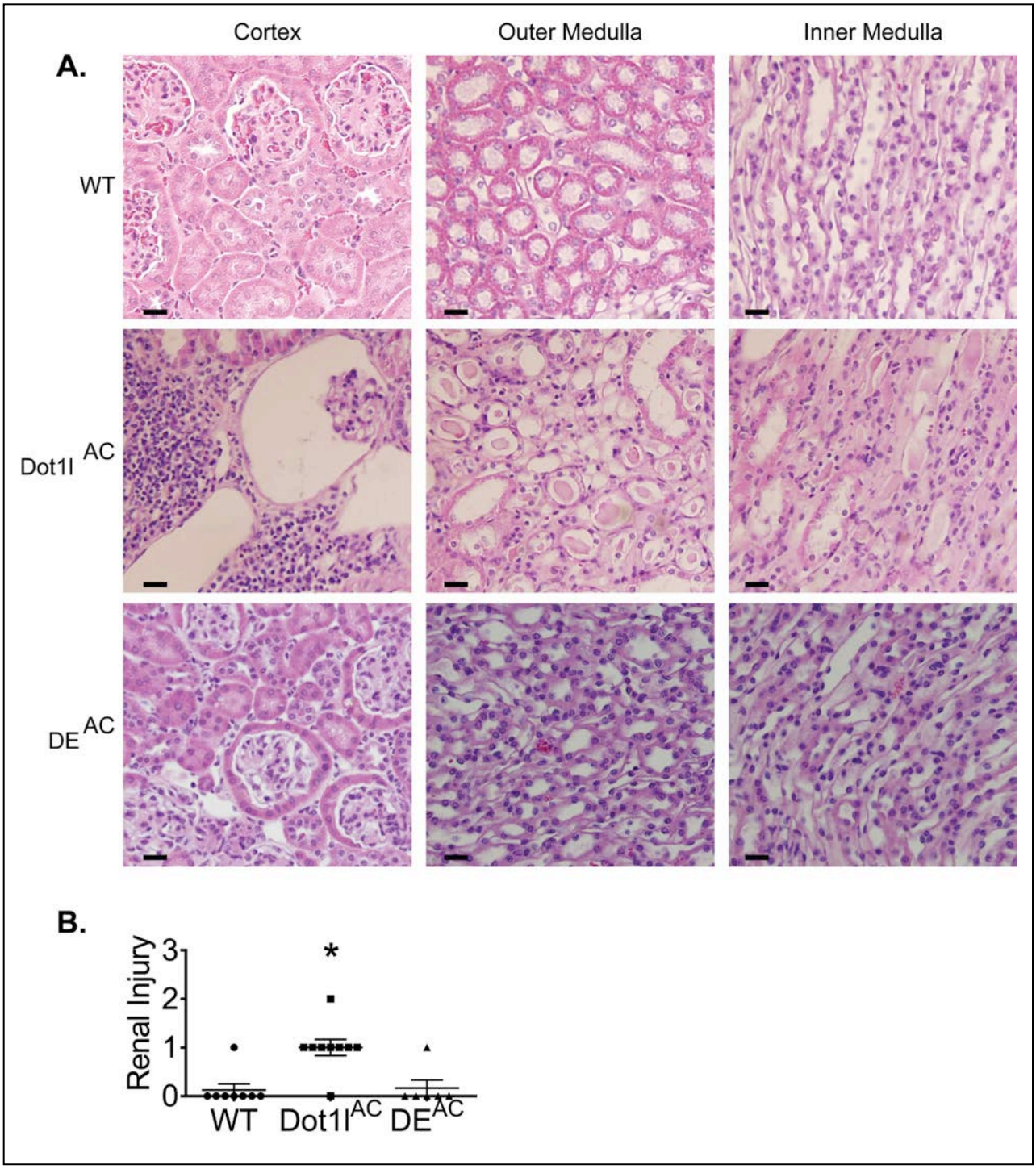
A.
Cortex
Outer Medulla
Inner Medulla
WT
Dot1l AC
DE AC
B.
Renal Injury
3
2
1
0
*
WT
Dot1l AC
DE AC

Fig. S2. *Dot1l* inactivation facilitates development of severe kidney fibrosis at the age of 14 months by upregulating ET1. A. H & E staining showing that WT mice had normal cortical parenchyma and lacked interstitial fibrosis/tubular atrophy or glomerulosclerosis. In the outer medulla, the loops of Henle and CDs showed no epithelial injury, hyaline casts, or interstitial fibrosis. In the inner medulla, CDs were lined by hobnailed epithelia with inconspicuous cytoplasm. The cortical parenchyma of *Dot1l*^{AC} mice, however, exhibited significant interstitial fibrosis/tubular atrophy with mononuclear inflammatory infiltrate in areas of scarring. Tubular epithelial injury was present, characterized by attenuation of epithelial cytoplasm. Glomeruli were shrunken with dilation of Bowman's space, indicative of atubular glomeruli and the global effect of *Dot1l* deletion. Since podocytes possess a fully functional ET system and represent a target of ET1, the glomerular shrinkage may result from the detrimental action of ET1. Epithelial cells in the outer medulla had reduced cytoplasm in the thick segments of loops of Henle and CDs, and hyaline casts in CDs. The inner medullary CDs exhibited clearing of cytoplasm of the epithelial cells lining CDs and focal hyaline casts. *DE*^{AC} animals showed no abnormalities in the cortex and attenuated cytoplasm without hyaline casts in the medulla. **B.** Semi-quantification of renal injury defined as tubular sloughing, cast formation, dilation, degeneration, atrophy, or tubulitis. n= 6-9 mice/group. *: $P<0.05$ vs. WT. #: $P<0.05$ vs. *Dot1l*^{AC}.

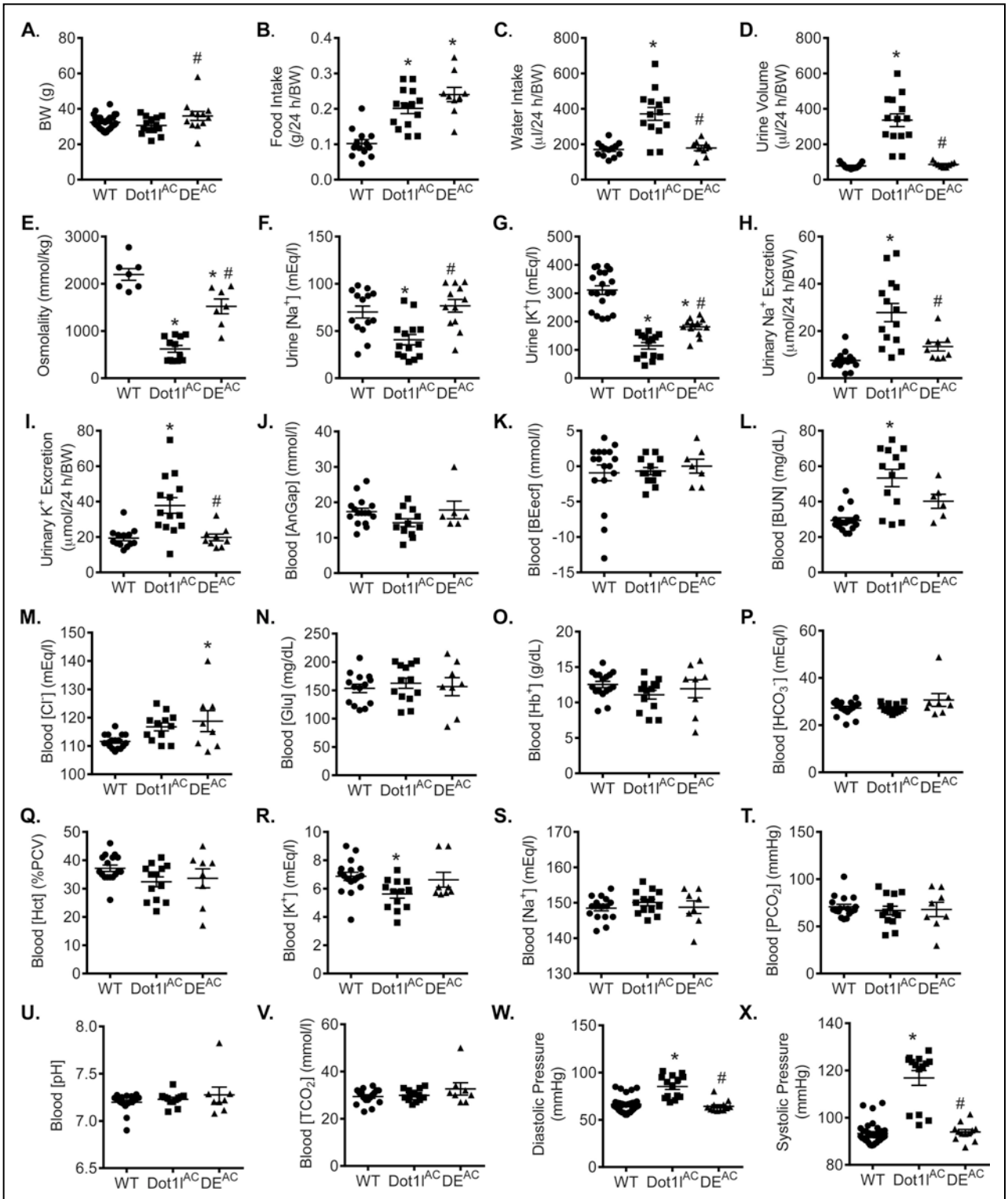

Fig. S3. *Dot1l* inactivation facilitates kidney malfunction during normal aging by upregulating ET1. Mice at the age of 14 month were analyzed for the parameters as indicated. n=6-34 mice/group. In all cases, *: P<0.05 vs. WT. #: P<0.05 vs. *Dot1l*^{AC}.

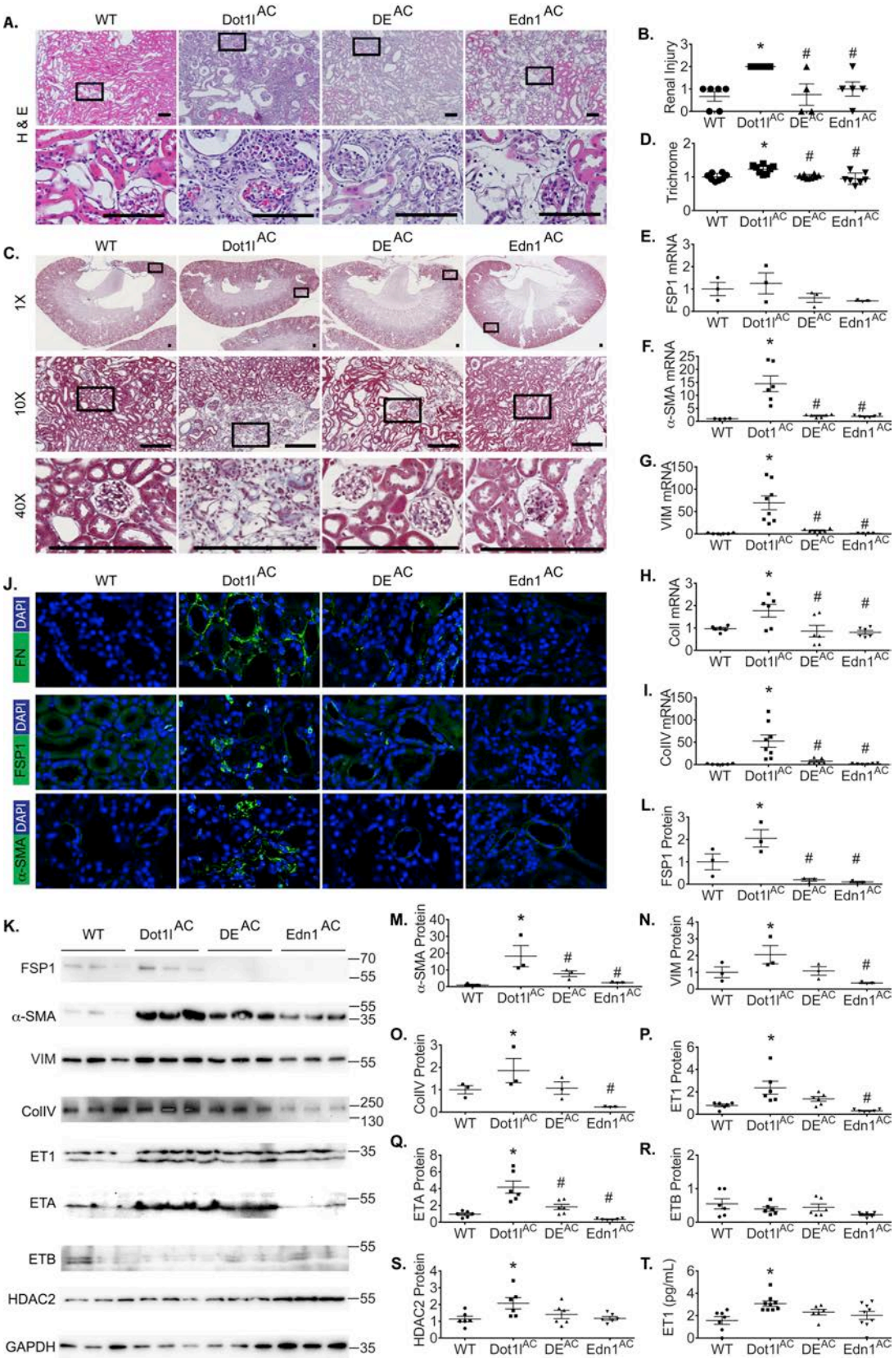
A.
WT
Dot1l AC
DE AC
Edn1 AC
H & E
B.
Renal Injury
C.
1X
10X
40X
D.
Trichrome
E.
FSP1 mRNA
F.
α-SMA mRNA
G.
VIM mRNA
H.
ColI mRNA
I.
ColIV mRNA
J.
DAPI
FN
FSP1
α-SMA
L.
FSP1 Protein
K.
FSP1
α-SMA
VIM
ColIV
ET1
ETA
ETB
HDAC2
GAPDH
M.
α-SMA Protein
N.
VIM Protein
O.
ColIV Protein
P.
ET1 Protein
Q.
ETA Protein
R.
ETB Protein
S.
HDAC2 Protein
T.
ET1 (pg/mL)

Fig. S4. *Dot1l* ablation exacerbates STZ-induced kidney fibrosis by upregulating ET1. Mice at the age of 2 months were injected IP with a single dose of STZ (150 mg/kg) and examined 4 months later. **A & B.** HE staining (A) and renal injury score (B) showing the lack of obvious abnormality in WT mice. In contrast, chronic tubulointerstitial injury characterized by focal mesangial expansion and hypercellularity, zonal interstitial fibrosis and tubular atrophy with sparing of glomeruli was evident in $Dot1l^{AC}$. This phenotype was significantly ameliorated in DE^{AC} and $Edn1^{AC}$ mice. n= 4-6 mice/group. **C & D.** Masson's Trichrome staining images (C) and ImageJ-based quantification of the staining (D) showing a significantly higher level of kidney fibrosis than the other three groups. Boxed areas in 1X were sequentially 10X and 40X magnified. n= 7-8 mice/group. Each point represents the average of 3-4 independent measurements of the entire kidney of the same mouse. The intensity was normalized to WT. **E**-**I.** Real-time RT-qPCR of the whole kidney showing mRNA expression of the genes as indicated. n=4-8 mice/group. **J.** IF showing expression of 3 fibrotic markers (green). **K**-**S**. IB analyses of the whole kidney as indicated, with GAPDH for normalization. The 35-kd band in the ET1 blot was considered to be non-specific and was excluded from quantification. n=7-8 mice/group. **T.** ELISA showing plasma ET1 levels. n=6-9 mice/group. In all cases except **T**, quantitative data were normalized to WT. Scale bar: 200 μm. *: $P<0.05$ vs. WT. #: $P<0.05$ vs. $Dot1l^{AC}$. $: $P<0.05$ vs. DE^{AC}.

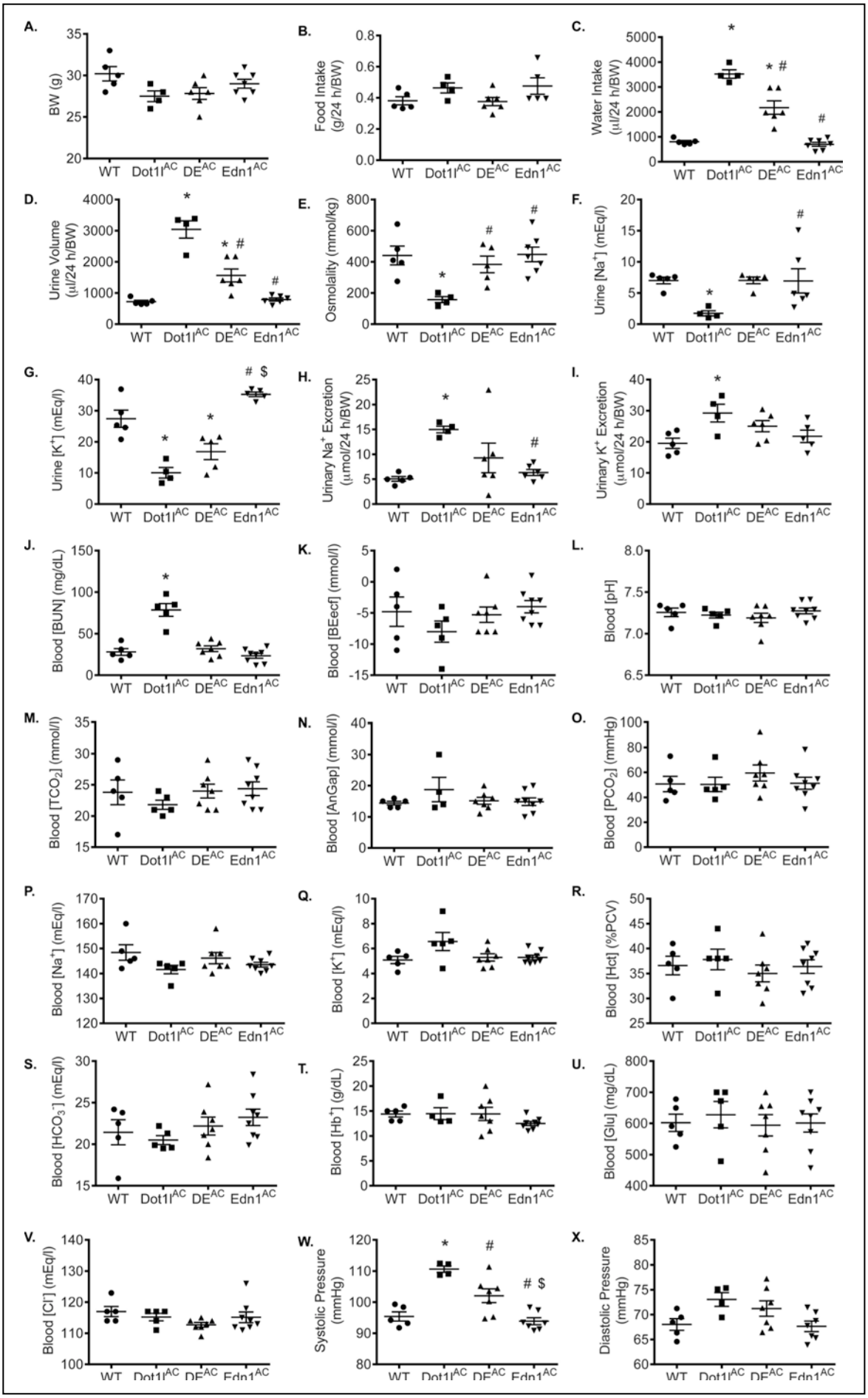
A.
BW (g)
B.
Food Intake (g/24 h/BW)
C.
Water Intake (µl/24 h/BW)
D.
Urine Volume (µl/24 h/BW)
E.
Osmolality (mmol/kg)
F.
Urine [Na+] (mEq/l)
G.
Urine [K+] (mEq/l)
H.
Urinary Na+ Excretion (µmol/24 h/BW)
I.
Urinary K+ Excretion (µmol/24 h/BW)
J.
Blood [BUN] (mg/dL)
K.
Blood [BEecf] (mmol/l)
L.
Blood [pH]
M.
Blood [TCO2] (mmol/l)
N.
Blood [AnGap] (mmol/l)
O.
Blood [PCO2] (mmHg)
P.
Blood [Na+] (mEq/l)
Q.
Blood [K+] (mEq/l)
R.
Blood [Hct] (%PCV)
S.
Blood [HCO3-] (mEq/l)
T.
Blood [Hb+] (g/dL)
U.
Blood [Glu] (mg/dL)
V.
Blood [Cl-] (mEq/l)
W.
Systolic Pressure (mmHg)
X.
Diastolic Pressure (mmHg)
WT
Dot1l AC
DE AC
Edn1 AC

Fig. S5. *Dot1l* loss exacerbates STZ-induced kidney malfunction by upregulating ET1. Mice at the age of 2 month were IP injected a single dose of STZ (150 mg/kg) and analyzed 4 months post the injection for the parameters as indicated. n=4-8 mice/group. In all cases, *: P<0.05 vs. WT. #: P<0.05 vs. $Dot1l^{AC}$. $: P<0.05 vs. DE^{AC}.

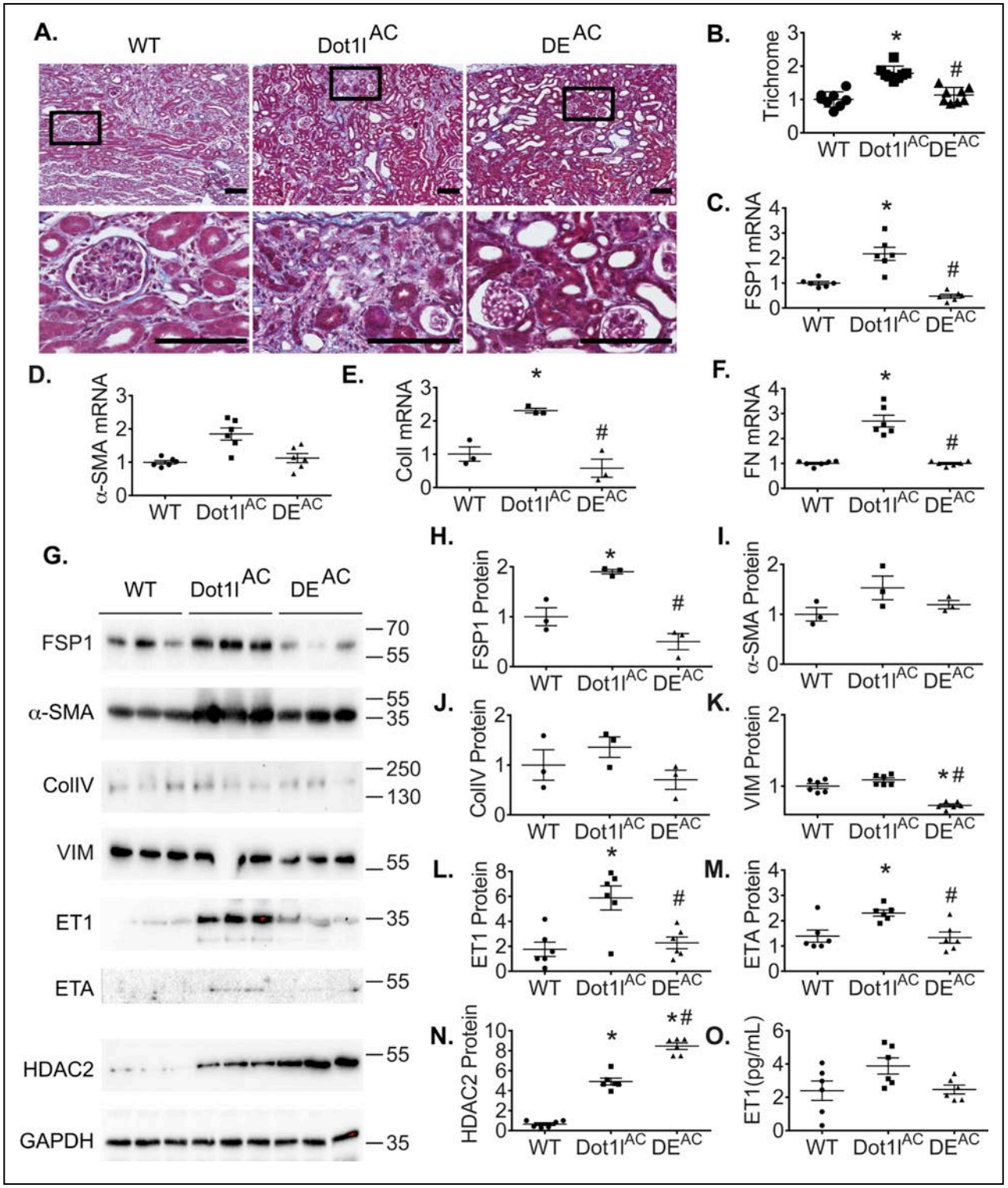
A.
WT
Dot1l AC
DE AC
B.
Trichrome
C.
FSP1 mRNA
D.
α-SMA mRNA
E.
ColI mRNA
F.
FN mRNA
G.
WT
Dot1l AC
DE AC
FSP1
α-SMA
ColIV
VIM
ET1
ETA
HDAC2
GAPDH
70
55
55
35
250
130
55
35
55
55
H.
FSP1 Protein
I.
α-SMA Protein
J.
ColIV Protein
K.
VIM Protein
L.
ET1 Protein
M.
ETA Protein
N.
HDAC2 Protein
O.
ET1(pg/mL)

Fig. S6 *Dot1l* ablation exacerbates UUO-induced kidney fibrosis by upregulating ET1. Two-month-old mice were subjected to UUO and examined 14 days after surgery. **A & B.** Masson's Trichrome staining images (A) and ImageJ-based quantification of the staining (B) showing a significantly higher level of kidney fibrosis in $Dot1^{AC}$ than WT or DE^{AC} mice. n= 8 mice/group. **C**-**F.** Real-time RT-qPCR of the whole kidney showing mRNA expression of the genes as indicated. n=7-8 mice/group. **G-N**. IB analyses of proteins in the whole kidney as indicated. GAPDH was used for normalization. The 35-kd band in the ET1 blot was considered to be non-specific and was excluded from quantification. n=3-6 mice/group. **O.** ELISA showing plasma ET1 levels. n=6 mice/group. In all cases except **O**, quantitative data were normalized to WT. Scale bar: 200 μm. *: P<0.05 vs. WT. #: P<0.05 vs. $Dot1l^{AC}$.

References for SI

1. Wu, H, Chen, L, Zhou, Q, Zhang, X, Berger, S, Bi, J, Lewis, DE, Xia, Y, Zhang, W: Aqp2-expressing cells give rise to renal intercalated cells. *Journal of the American Society of Nephrology : JASN,* 24**:** 243-252 2013.

2. Schmidt, RE, Dorsey, DA, Beaudet, LN, Frederick, KE, Parvin, CA, Plurad, SB, Levisetti, MG: Non-obese diabetic mice rapidly develop dramatic sympathetic neuritic dystrophy: a new experimental model of diabetic autonomic neuropathy. *The American journal of pathology,* 163**:** 2077-2091, 2003.